

Contributions to the development of crystal growth technologies

Peter Rudolph

Ceremonial lecture on the occasion of awarding of the Laudise Prize 2023

1. Introduction

In front of me is the book of Robert Alfred Laudise (1930 - 1998) “The Growth of Single Crystals” (New York: Prentice Hall, 1970). This is one of the first summary on crystallization methodology. Most of the major techniques and materials are reviewed and a pleasing amount of detail is associated with a substantial number of the growth methods described. In particular, numerous technological solutions from his own laboratory experiences, especially at the Bell Labs and MIT, are taught. It was the special merit of him to make clear the important role of technology in crystal growth. J. Gilman pointed out in his obituary: “Bob is an icon for crystal growth technology and a strong advocate for materials technology in general” [1]. In 1984 he was awarded the first experimental award of the International Organization of Crystal Growth (IOCG), which was then renamed the “Laudise Prize” in 1989 in his honor.

I first met him in person during the Sixth International Conference on Crystal Growth (ICCG-6) in 1980 in Moscow. At that time he represented the IOCG as President (1977-1983). I remember him as a very warm-hearted, helpful and humble person. As editor of the Journal of Crystal Growth he encouraged me and my co-authors as young researchers to submit a manuscript for our poster on growth of IV-VI compounds considering deviations from stoichiometry. Further we discussed the future efforts of IOCG to bring together more crystal growth groups of the world. Generally, his book, presentations and publications influenced me emphatically because of their methodological precision always in correlation with the fundamentals of crystallization. This has also become the principle of my more than 50 years technology-driven scientific life, about which I would like to show selected results here.

2. Shaped crystal growth

Shaped crystal growth refers to the growth of single crystals with a predetermined cross sectional configuration designed for a specific application. The quest to develop such techniques has been driven by the need to minimize costs associated with device fabrication such as cutting or polishing, the loss of expensive materials during these fabrication processes, and the damage created by machining processes [2]. Well known is the edge-defined film-fed

growth (EFG) [3] for the production of sapphire tubes, silicon ribbons, oxide filaments, and other shapes for special purposes, for example. I first came into contact with such considerations in 1967 as student of electronic technology in the laboratory for epitaxy at the Polytechnical University in Lviv (Ukraine). There was born the idea to obtain monocrystalline semiconductor layers of rectangular shape on insulator substrates by pressing a melt droplet into a shaping die (mask) by using a flap mechanism under inert gas and subsequent unidirectional solidification starting from a thin mask channel [4] (Fig. 1). We obtained various doped and undoped single crystalline layers of Te, Ge, III-V and II-V compounds of thickness 5 - 150 μm showing mirror like surfaces and low dislocation densities ($\sim 10^2 \text{ cm}^{-2}$). Such a piece was quasi ready for application as integrated device matrix and diverse energy converters.

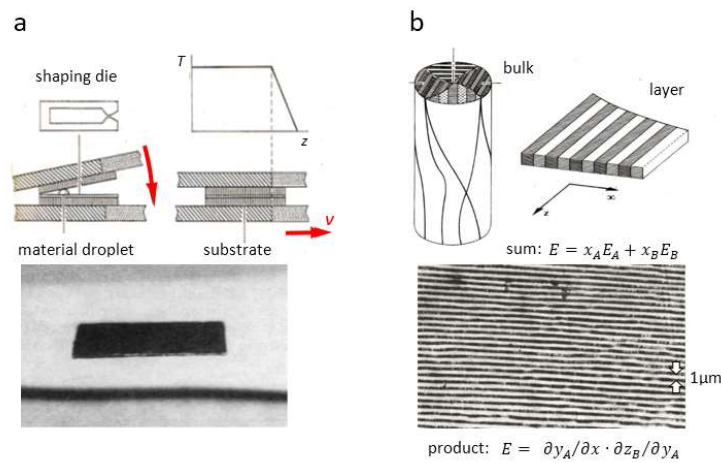


Fig. 1: Shaped growth of thin layers on substrates by pressing a melt droplet into a shaping die (mask) and subsequent unidirectional solidification in a temperature (T) profile by drawing with velocity v along z coordinate through a temperature gradient; **a** - shaping of semiconductor thin sheets on insulator substrates (the image shows a monocrystalline CdSb layer on a glass-ceramic substrate); **b** - comparison between conventional crystal growth in cylindrical shape and directional solidified layers of lamellar binary A-B eutectic structures usable for generation of sum and product properties with E - resulting effect, $x_{A,B}$ - respective portions of phases A,B, $E_{A,B}$ - partial phase property, $\partial y_A / \partial x$ - generation of response y_A to the input x in phase A, $\partial z_B / \partial y_A$ - generation of response z_B to input y_A from phase A into phase B (the image shows a tested Pb-Sn sheet with ordered superstructure). Adapted from ref. [5].

After obtaining my PhD and starting of my employment at Dept. of Crystallography of the Humboldt University in Berlin I introduced this technology to them. Following the idea of my adviser L. Ickert, this principle was used to produce eutectic layers with high ordered lamellar structure. Such superlattices are not achievable with melt bulk growth methods due to the cylindrical crystal shape leading to irregularly arranged eutectic grain structure (Fig. 1b). The interest in such ordered structures was caused by possible generation of sum and product properties which can be generated in strongly parallel aligned two different material phases. Various eutectic superlattices were obtained in many experiments with the participation of numerous students. More details are summarized in my book on profile crystal growth [5].

It is interesting to note that recently in 2022 a patent has been published by the Southampton University (GB) showing quite similar, but better elaborated methodical carrying out of the unidirectional solidification of molten alloy layers (e.g. $\text{Ge}_{1-x}\text{Si}_x$) in a mask between insulator substrates [6] (a reference to our formerly publications would be justified in the extensive bibliography).

Then the casting with subsequent unidirectional solidification of monocrystalline sheets of CdTe with an as-grown shape similar to the device profile for radiation detectors I applied in cooperation with located industry during my stay at the Institute for Material Research (IMR) of the Tohoku University in Sendai (Japan) from 1993 to 1994. Crystals with high resistivity of average value of $5 \times 10^9 \Omega \text{ cm}$ have been grown in dies of fused silica arranged in a vertical gradient freeze (VGF) furnace. No material loss by dissociation and, thus, no deviation from stoichiometry was obtained due to the total enclosure of dies [7].

At the same time in T. Fukuda's Laboratory I became acquainted with the EFG and micro-pulling down (μ -PD) growth of fiber crystals. For instance, the growth of in situ core doped laser rods by a double-die EFG was studied. In result, the relation between the core diameter and the inner die diameter, pulling rate, and meniscus height was derived [8] to guarantee a stable pulling-doping process. Using Cr and Nd as doping elements in LiNbO_3 rods the core with higher refractive index compared to the undoped rim region enables a more concentrated laser path by the cladding effect. A few years later, during a further stay at IMR, a joint book on fiber growth was published referring this important technological period [9].

From the very beginning of my new employment at the Institute for Crystal Growth in Berlin since 1994, I has been thinking about the saving of costly waste at the production of silicon solar cells from Czochralski (CZ) crystals. As it is well known the photovoltaic conversion efficiency of CZ-Si is still higher than multicrystalline solidified Si ingots. However, in order to obtain square solar wafers with edge lengths of 125 and 150 mm, conventional CZ crystals of cylindrical shape with diameters of 175 and 200 mm are needed, leading to cutting-related material losses of 25% and 28%, respectively. Thus, the growth of perfect CZ silicon crystals with quadratic cross section and, preferable, with reduced oxygen content, turned out to be a rewarding technological challenge for the crystal growers. Our team at that time in cooperation with industrial partner CaliSolar took on this task and tested the possibility to apply the kinetic principle of faceting (Fig. 2). The basic idea was to use the appearance of the four $\{110\}$ facets parallel to the $[001]$ pulling direction. For that, a very low and stable radial temperature gradient had to be achieved (Fig. 2a). With the help of numerical simulations it

was experimentally successful proved that a downward directed travelling magnetic field (TMF) of relative high frequency (300 Hz) generated in a coil-shaped heater around the crucible (see ch. 6) creates a favourable melt flow pattern supporting a highly stable temperature regime with very low radial temperature gradient along the melt surface and, thus, at the meniscus triple line [10]. As it is known, the common semiconductor materials with their covalent bonding tend to form facets during melt growth only on their most close-packed planes. After the Jackson criterion [11] in silicon the relation $\Delta h_{LS} / RT_m$ becomes 3.5 (with $\Delta h_{LS} = 50$ kJ mol⁻¹ the molar enthalpy of fusion, $R = 8.32$ J K⁻¹ mol⁻¹ the universal gas constant, and $T_m = 1683$ K the melt temperature). Then the surface anisotropy factor ξ_{hkl} to be multiplied decides that in silicon the {100} planes become atomically rough due to $\xi_{100} = 0.5$ ($\alpha \approx 1.7$), but the {111} and {110} faces atomically smooth with $\xi_{111} \approx 0.8$ ($\alpha \approx 3$) and $\xi_{110} \approx 0.6 - 0.7$ ($\alpha \approx 2.5$) [12], respectively.

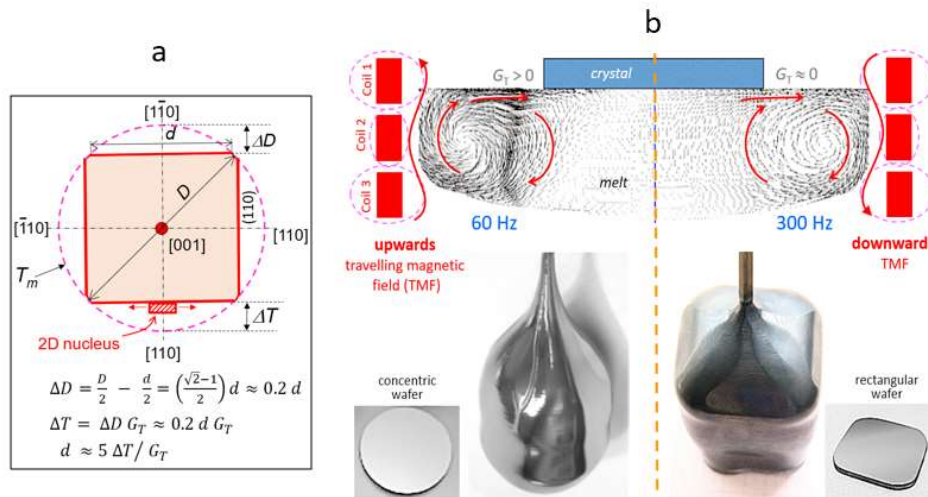


Fig. 2: Czochralski growth of silicon single crystals with rectangular cross section in a travelling magnetic field (TMF) generated within the coil-shaped heater; **a** - calculation of the {110} facet width d as function on the radial temperature gradient G_T with T_m - melting point isotherm, ΔT - supercooling necessary for 2D nucleation of the {110} planes, D - diagonal of the desired quadratic cross section; **b** - comparison between two different TMF parameters inducing contra-rotating melt vortices as a condition for concentric or rectangular crystal cross section [10].

According a simple geometrical consideration the relation between the facet length d and maximum undercooling at the facet centre ΔT necessary for two-dimensional nucleation is $d \approx 5 \Delta T / G_T$ with G_T the radial temperature gradient perpendicularly to the facet (Fig. 2a). Assuming the maximum undercooling of near dislocation-free {110} Si faces of ~ 2 K and a radial temperature gradient $G_T \approx 1$ K cm⁻¹ a facet width of ≈ 10 cm can be expected. Indeed, we have been successful in pulling tests of Si single crystals with reproducible square cross sections of about 91 x 91 mm² up to lengths of 10 cm (image right below in Fig. 2b).

Additionally was found a minimum of oxygen concentration of $7.5 \times 10^{17} \text{ cm}^{-3}$ along the cross section diagonal [13]. Geometrically well-shaped wafers have been obtained by equidistant dissection of the as-grown crystal bodies without considerable material loss. This research result is ready for further optimization and possible application

3. Influence of melt structure on II-VI crystal quality

Single crystalline semiconductor II-VI compounds, especially CdTe and mixed crystals ($\text{Cd}_{1-x}\text{Zn}_x\text{Te}$), are of eminent importance for production of X- and γ -ray radiation detectors as well as infrared devices. However, compared with III-Vs the successful growth of II-VIs from the melt is much more difficult due to their extremely complex material parameters. These include the very low thermal conductivity, minimal stacking fault energy responsible for high twinning probability, and, in particular, the high percentage of the ionicity in the bond energy ($\sim 72\%$). As it is well known the higher the bond ionicity f_i of a given material system the higher is the degree of association α_d within the fluid phase [14]. For instance, the molten state of III-V compounds with low f_i values $< 40\%$, like GaAs, GaSb, and InSb, show metallic character with very low α_d (< 0.1) in the melt. Thus, dissociated III and V atoms are presented immediately during melting and, therefore, are incorporated as separated building units at the crystallization front which is the preposition of assembling a well-ordered crystal lattice in accordance with each predetermined seed orientation. However, another situation occurs in compounds of high ionicity, such as II-VIs (CdTe, ZnTe, ZnSe), showing a degree of association (> 0.95) and still semiconducting behavior of the melt [15]. In such case an associated melt of preserved tetrahedral coordination, slightly fluctuating with time, meets the crystallization front. Hence, contrary to the disorder-order transition in III-Vs a quasi ordered-order transition occurs in II-VIs (in 1994 I discussed helpfully this phenomenon with A. Chernov who studied the situation of diffuse interfaces consisting of quasi preordered melt [16]). As a result, the highly associated building units of the melt are incorporated into the solid phase as such impressing the local orientation by their alignment. Then, an enhanced grain structuring is very obvious [17].

During numerous experiments of seedless vertical Bridgman growth of CdTe at the beginning of nineties together with my co-worker M. Mühlberg we observed that the quality of as-grown crystals is markedly dependent on the degree of superheating of the melt before the crystallization is started (Figs. 3a and 4) [18]. First, there is a distinct self-orientation mostly along $\langle 110 \rangle$ - $\langle 111 \rangle$ - $\langle 221 \rangle$ independently whether a seed is used or not [19] which was also found by other authors in CdTe, e.g. [20] and ZnSe, e.g. [21]. Thus, an oriented seed in

the $\langle 100 \rangle$ direction does not propagate but immediately changes the orientation toward above mentioned directions. Further, we found out, that an overheating of the melt $\Delta T^+ = T_m + (20 \dots 30)$ K, with T_m the melting point (CdTe: 1094 °C), proves to be a decisive factor to reduce the melt association and improve the crystal quality by marked lowering the number of large-angle grain boundaries and twins (Figs. 3a,c and 4) [22].

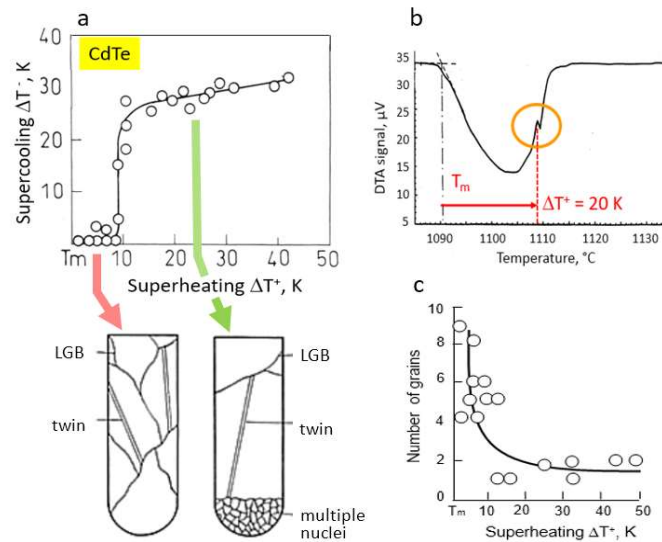


Fig. 3: **a** - degree of supercooling ΔT^- and structural quality of unseeded Bridgman and VGF grown CdTe crystals in dependence on the superheating ΔT^+ over the melt temperature T_m before crystallization; **b** - DTA showing a second minimum at superheating over T_m of 20 K; **c** - decreased number of large-angle grain boundaries (LGB) with increasing superheating of the Cd-Te melt (adapted from refs. [18,22,52]).

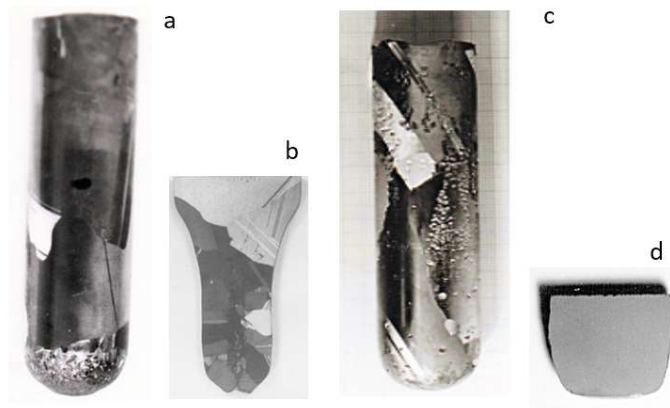


Fig. 4: Vertical Bridgman-Stockbarger seedless grown CdTe crystals from high (a,b) and low (c,d) superheated melts. **a,b** - crystallized after superheating $\Delta T^+ = 25 - 30$ K showing tips with spontaneously generated nuclei and relative sharp transition to nearly single crystalline structure; **c,d** - crystallized at very small superheating $\Delta T^+ = 2$ K showing no spontaneous nucleation, even sometimes monocrystallinity (d), but then a polycrystalline structure containing more LGBs and twins (adapted from refs. [18,22]).

Many following investigations (not only by the author's team) on the dependence of supercooling on the superheating and thermo differential analysis (DTA), like in Fig. 3b [23], strengthened our realization that these phenomena are strongly correlating with the high degree of ionicity retaining in the melt at small superheatings. Substantial evidence of this was

provided by the neutron scattering measurements on small overheated CdTe and ZnTe melts showing characteristic fourfold coordination typical for tetrahedral structure [24]. The same result was achieved by MC and MD numeric modeling [25,26].

Meanwhile, the supplies of CdTe and (Cd, Zn)Te crystals from well-overheated melt either by self-nucleating Bridgman growth with moving melt container from a hot zone into a cold one or vertical gradient freeze by moving the desired temperature gradient in a furnace via temporal change of power became the worldwide production standard. Even an artificial $\langle 110 \rangle$ seed proved to be successful [27]. Low defect CdTe crystals were grown during my stay at the Autonomous University of Madrid by applying a longitudinally rotatable Bridgman furnace allowing in the first step to overheat the melt until $\Delta T^+ = 110$ °C by keeping the CdTe seed below the melting point in the cold ampoule region. In the second step the melt temperature was lowered up to $\Delta T^+ = 8 - 13$ °C over the melting point and the seed was contacted and partially remelted by furnace rotation in order to start the growth process [28].

To overcome the above mentioned complications of the growth from melt currently the travelling heater method (THM) [29] from Te-rich melt-solution at lower process temperature (about 750 - 800 °C) and, therefore, higher stacking fault energy has proven to be the favored method [30, 31]. Note, also the authors team contributed to this technology by earlier methodical basic research [32, 33, 34].

4. Stoichiometry control to reduce intrinsic point defects and 2-nd phase content

As is well known, at all temperatures T above absolute zero, thermodynamic equilibrium concentrations of intrinsic point defects n_i (vacancies, self-interstitials and, in compounds antisites) will exist. This is because point defects n_i increase the configurational entropy of the regular crystal lattice that contributes to the decrease of its free Gibbs energy [35]. Due to $n_i \sim \exp(-1/T)$ in compounds $A_{\nu_A} B_{\nu_B}$ ($\nu_{A,B}$ - integers of stoichiometry) with increasing T the soaring intrinsic point defect density enlarge the region of compound existence via deviation from stoichiometry $\delta_{A,B}$ according $A_{\nu_A \pm \delta_A} B_{\nu_B \mp \delta_B}$. Hence, the boundary of the existence region, named solidus of the AB compound, is retrograde with decreasing T [36].

These fundamental facts are of decisional consequences for compound and mixed crystal growth from the melt. This includes, that at high temperatures in the growing crystal the point defects, exhibiting high thermal oscillation energy, are isolated and usually electrically charged that promotes their interacting with each other and with presented charged extrinsic

point defects (residual impurities, dopants). As a result, defect complexes are formed influencing the Fermi energy level considerably. Further, due to the retrograde solidus of the region of compound existence during the cooling process the native point defects, like interstitials and vacancies, condensate in harmful precipitates and microvoids, respectively. Additionally, the splitting between solidus and liquidus on both sides of the congruent melting point implicates the effect of segregation responsible for a diffusion boundary layer of the excess component A or B at the propagating melt-solid interface. This may result in an incorporation of inclusions at the smallest interface instability or exceedance of the solubility limit within the diffusion boundary layer. Therefore, we have to deal with two different origins of second phase particles, i.e. condensation of *precipitates* with usually very small diameter between 10 -100 nm mostly decorating presented dislocations, and incorporation of *inclusions* with larger diameter between 1- 50 μm [37] (Fig. 5).

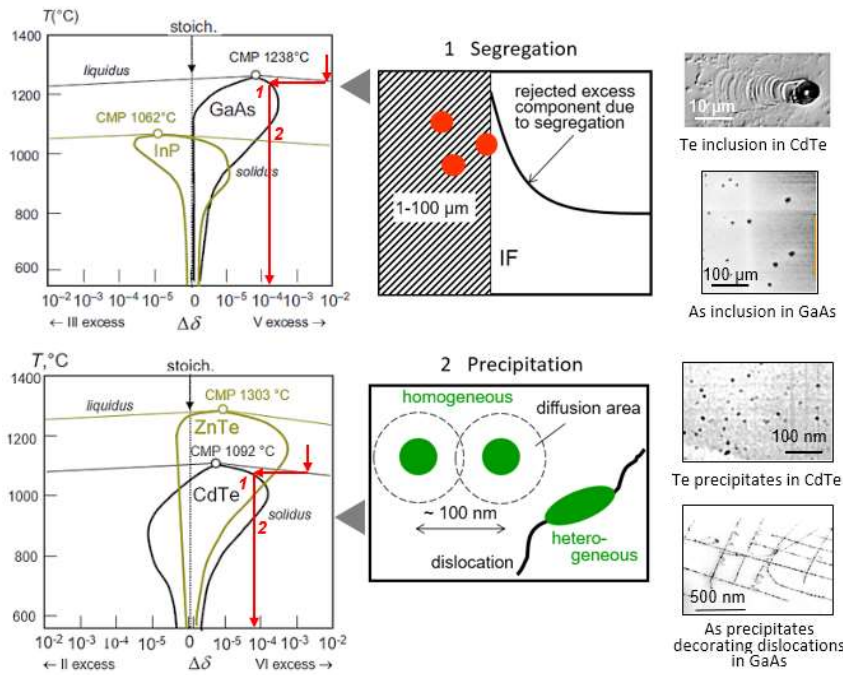


Fig. 5: Sketches of the homogeneity regions of selected III-V and II-VI compounds with crystallization paths at the growth from non-stoichiometric melt. Deviating from the congruent melting point CMP (point 1) the effect of segregation takes place leading to formation of a diffusion boundary layer and possible incorporation of excess components as inclusions. Due to the retrograde solidus in the cooling crystal (point 2) precipitates are nucleated decorating presented dislocations. The images right show Te and As inclusions and precipitates in CdTe and GaAs, respectively, which markedly differ by their size (see e.g. ref. [37]).

In close cooperation with my teams I studied extensively the origins, correlations and control of the above mentioned phenomena, especially at III-V (GaAs, InP) and II-VI (CdTe, ZnSe) compound growth. For instance, it was shown that the concentration of electrically active doping elements depends on the deviation from stoichiometry. Using photoluminescence

analysis, mass spectroscopy and atomic absorption spectrophotometry on CdTe crystals doped with Ag, Cu or P it was found that the concentrations of substitutional acceptors, e.g. Ag_{Cd} , and donors, e.g. P_{Te} , are controlled by the density of Cd and Te vacancies at the growth temperature, i.e. the deviation from stoichiometry, respectively [38]. That means, one is the thermodynamic distribution coefficient $k_0 = x_S^i/x_L^i$, with $x_{S,L}^i$ the mole fraction of the given dopant i in the solid S and melt L , but the other is the incorporation coefficient for substitution $k_i = x_{V_S}^i/x_L^i$ of provided free vacancy sites in the solid $x_{V_S}^i$. Because it was found that $k_i < k_0$ one can assume that the incorporated but not substituted and, thus, electrically neutral dopant excess is concentrated in tellurium inclusions attracting foreign atoms during their still liquid state during cooling process [39].

An important tool for the achievement and study of point defect state, structural crystal quality and second particle content is the melt growth with in situ control of the stoichiometry or well-defined deviation from it by an in situ vapor partial pressure source of the volatile component. This was applied for CdTe by vertical and horizontal Bridgman techniques with Cd source [22, 40], for ZnSe by high-pressure vertical Bridgman and VGF with Zn source [41], and for GaAs by the vapor pressure controlled Czochralski (VCz) growth with As source with and without B_2O_3 encapsulant [42]. The difference of the observed transition point between electron and hole concentration as function on the Cd source temperature in vertical and horizontal Bridgman growth [22,3939] made it clear to me that an exact thermodynamic three-phase equilibrium can be only obtained, when both the solid phase boundary of the growing crystal and the adjacent melt simultaneously contact the vapor phase. This is only the case at horizontal Bridgman and VCz growth. In comparison, at the vertical Bridgman growth and VGF the crystallization front is totally covered by the melt column having no direct contact with the vapor. Hence, to obtain the required melt composition at the growing interface the vapor pressure must be adapted to the local A/B relation depending on the degree of vapor-liquid separation at the melt surface, the diffusion- and convection-driven concentration level within the melt and the melt-solid segregation at the propagating interface. Using thermodynamic phase relationships I derived a balanced growth velocity for in situ pressure controlled vertical Bridgman growth and VGF (the mathematical details are given in refs. [22,3939]). A good experimental agreement was found. For example, for near stoichiometric growth of CdTe by vertical Bridgman technique with a growth rate of about 1 mm h^{-1} and vertical temperature gradient at the interface of 8 K cm^{-1} an extra Cd source temperature of about 1123 K ($850 \text{ }^\circ\text{C}$) was obtained confirming a relative weak melt convection. In a recent paper the near stoichiometric growth of $\text{Cd}_{0.8}\text{Zn}_{0.2}\text{Te}$ at axial temperature gradient at the interface of

$\sim 1 \text{ K cm}^{-1}$ and mean growth velocity of 1 mm h^{-1} was achieved by the Cd source temperature of 1123 K (825 °C) resulting in the lowest second phase Te particles within the CdTe matrix [43]. This result is not contrary to my estimations for CdTe because the Zn content reduces the difference between the solidus crossing the stoichiometry and liquidus whereupon a smaller Cd excess in the melt is required.

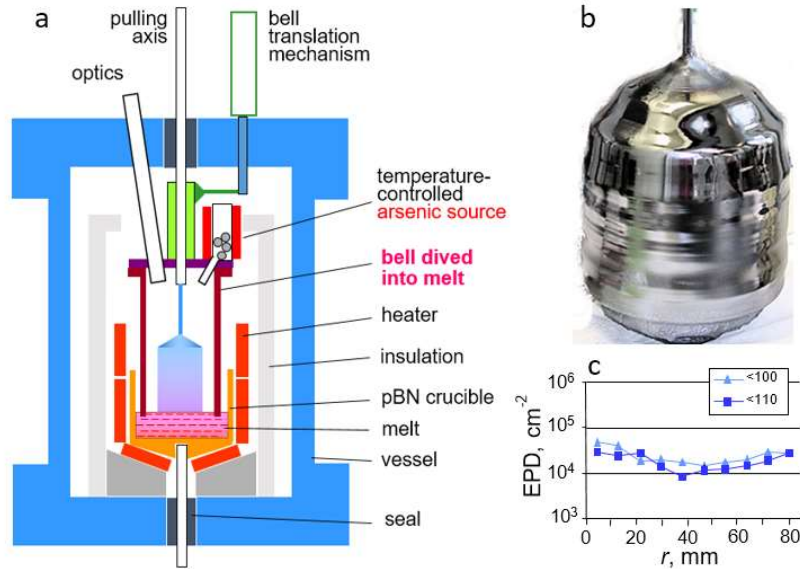


Fig. 6: **a** - Schematic of the VCz method with a bell diving into the melt without liquid encapsulation. The bell inside atmosphere is controlled by arsenic overpressure; **b** - as-grown semi-insulating 6-inch GaAs crystal with total length of 220 mm and mass of 18.2 kg grown by VCz showing mirror-bright surface without any features of As dissociation; **c** - etch pit density (EPD) along the radius r (adapted from refs. [44]).

New insights have been gained by using the VCz growth, actively co-developed by M. Neubert [42] for 6 inch GaAs crystals and realized by a bell around the growing crystal diving into the encapsulation layer or even into the melt even by omitting B_2O_3 encapsulant whereupon the inside atmosphere within the bell was controlled by an arsenic overpressure [44] (Fig. 6). First, all crystals of 22 cm length showed a mirror-bright surface (Fig. 6b) due to the depressed As dissociation even in reduced axial temperature gradients. A slightly convex growth interface was obtained responsible for higher radial homogeneity of electrical parameters and dislocation density distribution. Due to the reduced thermomechanical stress [42] the mean etch pit density (EPD) was much lower than in conventional GaAs LEC crystals, i.e. 10^4 cm^{-2} (Fig. 6c). Using a VCz arrangement with an inner As-controlled chamber around the melt crucible GaAs crystals have been grown by the team member F. Kiessling from Ga-rich and stoichiometric melts without boron oxide encapsulation and with controlled carbon concentrations [45]. The low boron content in the undoped VCz crystals resulted always in higher Ga vacancy concentrations and lower Ga_{As} antisite (\equiv EL2 defect) content compared to standard GaAs material. As a result, the growth of near-stoichiometric semi-insulating (SI) GaAs

crystals from Ga-rich melts with an as-grown resistivity of $1.14 \times 10^8 \Omega\text{cm}$ and an electron mobility of $5370 \text{ cm}^2 \text{ V}^{-1}\text{s}^{-1}$ at a melt mole fraction of $y = 0.46$ proved to be feasible. Beside the suppression of scattering As precipitates the absorption coefficient of boron-reduced VCz GaAs crystals grown from Ga-rich melts was much lower compared to boron-contaminated standard LEC and VGF GaAs crystals making such material favorable for use as windows, lenses and prisms in transmission optics for IR and THz frequency ranges.

Today, semi-insulating GaAs crystals for high-frequency communication are produced by VGF and vertical Bridgman method which proved to be more economical than the relative complex VCz technique [46]. However, I do not believe that last word on its have been spoken yet. There are many further materials, such as CdTe and InP, even with higher twinning probability, polycrystalline nucleation and impurity incorporation at solidification generated at the conducting container walls. Also many oxide melts show high component dissociation and, thus, precipitates and foreign phases without in situ pressure control. For example, I advised an industrial study at Carl Zeiss Jena of in situ stoichiometry controlled PbMoO_4 Czochralski crystals with an additional temperature controlled MoO_3 source within the growth chamber [47]. Characteristic PbO and Pb_2MoO_3 inclusions in standard uncontrolled crystals leading often to cracking have been successfully depressed by VCz technology. Furthermore, recently the growth of defect-reduced 6-inch InP LEC crystals within a dived bell was reported [48].

5. Study of dislocation cell patterning in as-grown crystals

An essential structural problem that occupies the crystal growers for a long time is the dislocation cell patterning in as-grown crystals and epitaxial layers regardless of the selected phase transition. This phenomenon is most researched in metallurgical load processes and intensive theoretically studied by the metal physicist [49]. Also in growing single crystals and heteroepitaxial layers dislocation patterning correlates with thermomechanical and misfit stresses, respectively. At the bulk growth such dislocation structuring impair the device quality obtained from. For instance, in semi-insulating GaAs wafers the sell structure demonstrated in Fig. 7a is responsible for fluctuation of the electrical resistivity, in CdTe radiation detectors the electron collection density is oscillating, and in multicrystalline silicon solar cells the planar internal quantum efficiency is unsteady distributed. Unfortunately, compared with metal physics in the crystal growth fundamentals the study of this phenomenon is still underdeveloped. Therefore, within the nineties we started an intensive investigation of the origins and engineering of dislocation cell patterning during growth of GaAs, InP, CdTe, mc-Si

and CaF_2 . The results are presented in numerous review papers [35, 50, 51, 52, 53] so that here the listing of most significant conclusions shall be sufficient.

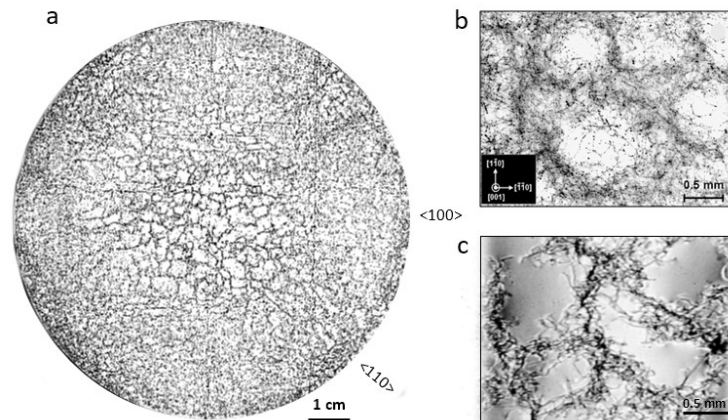


Fig. 7: Cellular structure in as-grown semiinsulating VGF GaAs crystals (adapted from ref. [35]); **a** - KOH etched 4 inch (100) wafer showing largest cells within the core section where the lowest thermomechanical stress of 0.5 MPa near the growing interface was numerically modelled. In comparison, in the rim region the stress was calculated to be 1.8 MPa (see e.g. [59]); **b** - cell structure analysis by laser scattering topography (adapted from ref. [55]); **c** - synchrotron X-ray topography showing giant cells free of dislocations interiors taken by the cooperating team of T. Tuomi et al. (Helsinki University).

Principally, dislocations are metastable defects with high energy. Their density cannot be drawn from equilibrium thermodynamics only. The thermomechanical work done during plastic flow is mainly dissipated into heat and the rest is stored in the form of elastic dislocation energy. Actually, such process should be far from thermodynamic equilibrium and promote spontaneous forms of self-organization (*dissipative structures*), such as cellular dislocation patterns. In growing bulk crystals the formation of such dislocation cells is realized immediately behind the crystallization front assisted by the acting thermomechanical stress. Essential condition proves to be the combination between dislocation glide, including cross glide, and climb assisted by high-temperature intrinsic point defect diffusion in order to generate the characteristic three-dimensional globular cells (note, the nearly missing cell structuring in growing InP crystals indicates a very small region of existence, i.e. relative low intrinsic point defect content). In addition to high-temperature climb processes, during cooling of thermomechanically stressed crystals the formation of small-angle grain boundaries by dynamic polygonization takes place. This phenomenon is based on long- and short-range interaction forces between presented dislocations resulting in their annihilation and accumulation in walls of remaining dislocations with similar Burgers vector [54]. Both processes of dislocation dynamics (DD) cause the reduction of the crystal enthalpy. In particular, at the arrangement of dislocations in walls the energy gain of each dislocation amounts to $\sim 25\%$. It is noteworthy that one has to differ between climb-assisted globular dislocation cell structuring and

small-angle grain boundary formation by dynamic polygonization, and, of course, especially large-angle grain boundaries due to multi-crystalline growth [53].

By the way, also at the growth of standard dislocation-free silicon crystals thermomechanical stress and intrinsic point defect diffusion are acting. However, the formation energy for dislocation generation shows too high (in the region of GPa) so that the stored energy is consumed to a large extent for intrinsic point defect agglomeration. But in the case of presence of dislocations, like in the case of directional solidification of multicrystalline silicon (mc-Si) ingots, cell structuring is also occurring (see image in Fig. 8) although the much higher critical resolved shear stress (CRSS), responsible for dislocation movement and multiplication, than in semiconductor compounds.

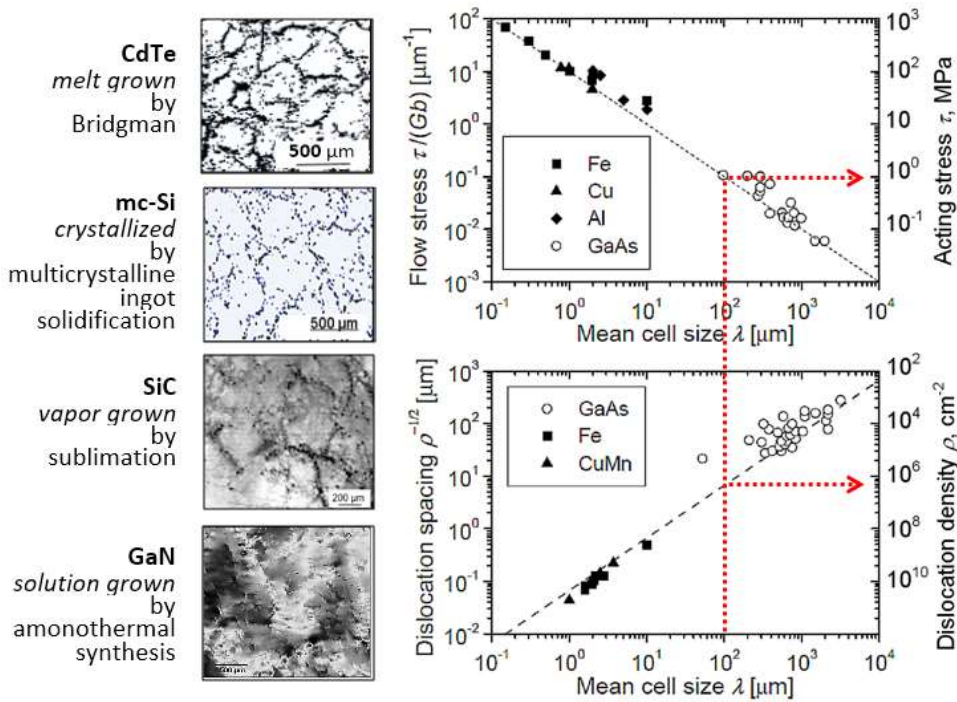


Fig. 8: The rules of correspondence of cellular patterning of dislocations in as-grown crystals independently on the crystallization method and material. The images show revealed dislocation cells in various crystals (adapted from [50,51]; the GaN image indicates X-ray Rocking curve imaging of cells by Caliste et al., *Microelec. Eng.* 276 (2023) 11201). The graphical functions show the dependence of cell diameter λ on acting stress τ (rule of Kuhlmann-Wilsdorf; see text) and dislocation density ρ (rule of Holt; see text). Bold symbols represent load tests on metals and empty symbols the numerically modelled thermomechanical stresses in growing VGF GaAs crystals. Cell dimensions and mean dislocation densities were revealed by etching after growth. The broken red lines illustrate how one can conclude from observed cell diameter in as-grown crystals (e.g. 100 μm) on the dislocation density ($\sim 10^6 \text{ cm}^{-2}$) and acting stress during crystallization ($\sim 1 \text{ MPa}$), respectively.

The spatial character of dislocation cells we revealed by the depth integration laser scattering topography in GaAs crystals [55] (Fig. 7b). The dislocation manner within the cell walls were analyzed by synchrotron X-ray topography [56] (Fig. 7c). Though, the question arose which stress strength is acting in the growing crystal and how the cell dimension is correlating with it. Because of the impossibility of direct measurement of the thermomechanical

stress in a growing crystal from from my team-mate Ch. Frank-Rotsch was used the 3D global numeric computer simulation of the von Mises stress components by inserting the presented temperature field during growth into the related thermoelastic strain equation [57] by applying the code CrysVUN++ [58]. Then, the obtained stress values together with the mean cell diameter, determined from the cross-sectional etched 2D cut by the stereological method [59], were inserted into the rules of correspondence (Fig. 8). At first, after Holt's relation the cell diameter λ is linked to the dislocation density ρ according $\lambda \approx \kappa \rho^{1/2}$ with κ - factor of proportionality amounting in the literature between 7 and 20. Then, the acting shear stress τ was estimated according to the rule of Kuhlmann-Wilsdorf $\tau = \kappa G b \lambda^{-1}$ with G - shear modulus, and b - Burgers vector. These relations have been observed by numerous load experiments of many materials, mainly metals [60] (see Fig. 8). My team found out a near similar behavior in growing semiconductor crystals by using $\kappa \approx 10$ [52,53] independently on much larger cell dimensions in as-grown single crystals due to suffering much lower thermal stress than in mechanically high-stressed metals as it is shown in Fig. 8. In this way, it is now possible to conclude from the measurable cell dimension by EPD to the mean dislocation density and acting stress force at high process temperature behind the interface (red lines in Fig. 8).

How to prevent such dislocation cell structures? Due to the dissipative character of the dislocation dynamics this is not an easy task. Nevertheless, we demonstrated that at near-stoichiometric growth conditions with in situ pressure control the cell structuring in GaAs could be minimized by reducing the atomic As excess and, therefore, the support for dislocation climb [61]. The same result can be reached by composition hardening adding an isoelectric mixing component as it was demonstrated at melt growth of $\text{Cd}_{1-x}\text{Zn}_x\text{Te}$ and $\text{CdTe}_{1-x}\text{Se}_x$ [6222], for example. Generally, undercritical thermal stress obtained by clever hot-zone engineering resulting in near linear temperature gradients proves to be the main counteraction [52].

6. Melt growth under travelling magnetic field generated in a heater-magnet module

The present and future demands of industrial bulk crystal growth from the melt are concentrated on improved crystal quality, increased yield, and reduced costs. To meet these challenges, the size of the melt volume must be markedly increased. As a result, violent convective perturbations appear within the melts due to turbulent heat and mass flows. They disturb the single crystal growth and give rise to compositional inhomogeneities. Thus, the application of external force fields proves to be an effective method to dampen and control these

flows and optimize the shape of the melt-solid interface. There are various stabilizing variants, such as constant and accelerated melt rotation, mechanical (ultrasound) melt vibration, electric current, and magnetic fields [63]. Especially nonsteady fields became very popular because, in this case, the needed strength of the magnetic induction is lower than for steady fields and the control parameters are more versatile [64].

In 2005 I was encouraged to apply a low-energy low-cost technology that combines heat and magnetic field generation in the heater placed close to the melt crucible [64]. This was the beginning of the considerable government-funded technological project KRISTMAG[®] at the institute for crystal growth (IKZ) Berlin in cooperation with numerous industrial and academic partners. It is important to emphasize that from the beginning the global numeric modeling, prior by N. Dropka, was included to find out the technological and efficient best way of realization (see e.g. [65]). Within the framework of these tasks internal heater-magnet modules for simultaneous generation of temperature and travelling magnetic fields (TMF) in diverse melt growth facilities have been developed and successfully tested in LEC pullers, VGF furnaces, and mc-Si ingot crystallizers (Fig. 9). Amplitude, frequency, and phase shift of the AC three-phase current are all adjustable and combined with a DC component for heating to control the crystallization set point. To obtain a vertically translating TMF, a multi-coil heater replaces the standard meandering “picket fence” heater shape as sketched in Fig. 9.

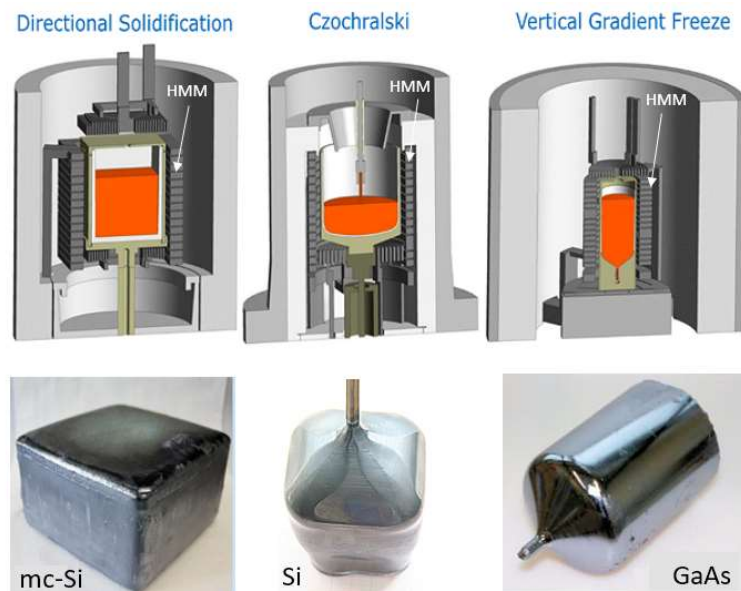


Fig. 9: Melt growth arrangements by applying TMF generated in a multi-coil heater via alternating current (AC) of given frequency and phase shift whereupon the required thermal field is produced by direct current (DC). Such furnace combination realized by the KRISTMAG[®] project at the IKZ Berlin is named heater-magnet-module (HMM) [64 - 66]. The TMF parameters for obtainment of rectangular Czochralski Si single crystals (middle image below) was already discussed in ch. 2 and published in ref. [13].

Recently a related review paper of the KRISTMAG[®] team of IKZ Berlin was published demonstrating the diversity of THM and successful results [65]. The possibility of obtainment of steady-state nearly zero radial temperature gradient at Czochralski growth in order to induce large side facets and, thus, rectangular cross section of the pulling crystal was already demonstrated in ch. 2 and shown in Fig. 2. Therefore, here few further examples will be referred only.

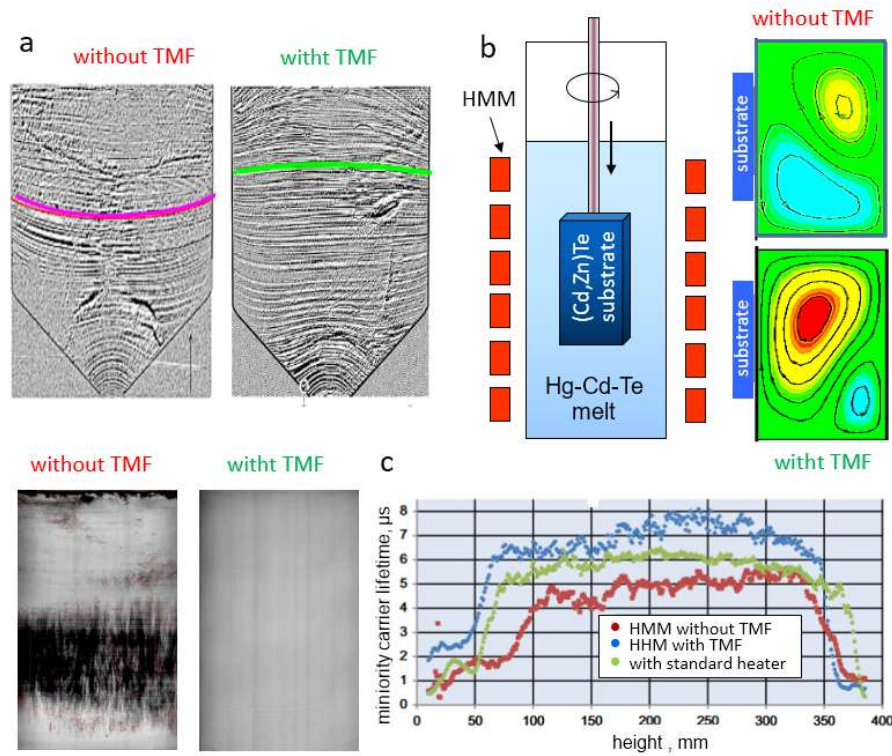


Fig. 10: Selected results of succesful application of TMF at the growth of semiconductor crystals, thin layers and multicrystalline ingots; **a** - the attainment of a slightly convex growing interface at VGF of germanium crystals where the temperature isotherm courses have been visualized by lateral photo voltage scanning on longitudinal cuts of the as-grown crystals (adapted from ref. [67]); **b** - vertical dipping LPE of $\text{Hg}_{1-x}\text{Cd}_x\text{Te}$ layers with strongly lamellar solution flow along the $\text{Cd}_{1-x}\text{Zn}_x\text{Te}$ substrate improving the parameter homogeneity of IR detectors (adapted from ref. [68]); **c** - improved IR transmission homogeneity and enhanced minority carrier lifetimes in 640 kg mc-Si ingots (adapted from ref. [69]).

First, TMF enables the tuning of a desirable slightly convex interface shape at the growth of germanium single crystals by VGF in order to obtain improved radial homogeneity of the physical material parameters like carrier concentration and mobility. The resulting temperature isotherms have been visualized for validation via striations by lateral photo voltage scanning (LPS) [66] on longitudinal cuts of the as-grown crystals. An example of the liquid-solid (L-S) interface shape of Sb-doped Ge single crystal is shown in Fig. 10 a. The unfavorable concave interface shape due to higher thermal conductivity in semiconductor melts than in the solid, known from the VGF standard process without magnetic field, could be optimized

toward a slightly convex one by the adjusted TMF with frequency $f = 20$ Hz and downwards phase shift $\phi = -90^\circ$. It was found, that a steady morphology of the growing L-S interface during the whole growth run must be controlled carefully by adapting TMF AC parameters in accordance with DC power [67].

Next, it was demonstrated that the use of the TMF in a furnace for vertical dipping LPE of $\text{Hg}_{1-x}\text{Cd}_x\text{Te}$ layers on fitting $\text{Cd}_{1-x}\text{Zn}_x\text{Te}$ substrates in Hg-Cd-Te melt-solutions improves markedly the thickness and parameter homogeneity of IR detectors manufactured according to this principle. Primarily the optimized TMF parameters were calculated by numeric simulation and it was found that a homogeneous convection vortex with steady lamellar flow along the substrate surface at a down phase shift of -120° and enhanced TMF frequencies of 100 - 400 Hz resulted in high $\text{Hg}_{1-x}\text{Cd}_x\text{Te}$ layer homogeneity (Fig. 10 b). After these very good experimental proofs the THM assisted LPE was translated to the industrial production [68].

Finally, for the first time a heater-magnet module was constructed, tested and translated to Schott Solar AG for directional solidification of mc-silicon ingots of industrial scale G5 (640 kg) [69]. The effective melt mixing and precise control of the interface shape demonstrated exhibiting superior properties of the ingots without affecting the stability of the Si_3N_4 crucible coating. The solidified ingots showed very homogeneous IR transmission without inclusions due to the reduction of the diffusion boundary layer by intense THM convection (Fig. 10 c). Due to the absence of inclusions the dislocation densities were somewhat decreased and their bunching was only rarely observed, resulting in overall high minority carrier lifetimes as shown in Fig. 10 c. The axial resistivity distribution, being inversely proportional to the boron concentration in the solidified silicon, showed a good agreement with Scheil's law [70] with a monotonic decline over the whole height of the ingot. Obviously boron was incorporated under conditions of complete melt mixing. In comparison, the resistivity curves of Si ingots solidified without a TMF showed non-uniformity with a series of flat and steep segments typically for insufficient and unsteady melt convection. Thus, the advantage of the KRISTMAG[®] concept for mc-Si solar cell production was clearly demonstrated [69].

Acknowledgement

Generally, successful achievements in technological developments are only possible in excellent teams composed of well complementary, harmonizing and talented theoreticians, engineers, modelers, and experimenters. This has always been the case in my more than fifty years of work and education in the field of crystal growth. Today I am very grateful to many

hardworking former advisers, coworkers and students at the laboratory of epitaxy at the Polytechnical University of Lviv, at the Dept. of Crystallography and Material Science of the Humboldt-University in Berlin, at the Institute for Material Research of the Tohoku University in Sendai, at the Leibniz Institute for Crystal Growth in Berlin, and many further institutes as well as numerous cooperating companies around the world. Most former excellent coworkers are listed in the common referred publications at the end of this paper.

Of the numerous industrial partners, I would like to highlight the cooperation with Freiburger Compound Materials GmbH. The main sponsors of our research include Bundesministerium für Bildung und Forschung (BMBF), Deutsche Forschungsgemeinschaft (DFG), Technologiestiftung Berlin (TSB), and European Union within the European Regional Development Fund (EFRE).

My special thanks goes to all those, especially, the members of the International Organization of Crystal Growth (IOCG) and German Association of Crystal Growth (DGKK) which recommended and decided to award me the high honorable Laudise Prize.

References

- [1] J.J. Gilman, Robert A.Laudise 1930-1998, in: Memorial Tributes: National Academy of Engineering, Vol. 10 (Nat. Academies Press 2002).
- [2] R.S. Feigelson, Growth of Shaped Crystals, in: H. Arend, J. Hulliger, J. (eds), Crystal Growth in Science and Technology. NATO ASI Series, vol 210 (Springer, Boston, MA1989) pp. 275.
- [3] H.E. LaBelle Jr, A.I. Mlavsky, Growth of controlled profile crystals from the melt: part II - edge-defined, film-fed growth (EFG), Mater Res Bull, 6 (1971) 581.
- [4] A.V. Sandulova, A.D. Goncharov, P. Rudolph, W. Thieme, L.D. Chutorjanskij, V.Ja. Schevchenko, Preparation of monocrystalline semiconductor thin layers by unidirectional crystallization of the melt between two substrates, Kristall und Technik 7 (1972) 787.
- [5] P. Rudolph, Profilzüchtung (Akademie verlag, berlin 1982).
- [6] Patent US11198951B2 (2021), Melt growth of single-crystal alloy semiconductor structures.
- [7] P. Rudolph, S. Kawasaki, S. Yamashita, Y. Usuki, Y. Konagaya, S. Matada, S. Yamamoto, T. Fukuda, Casting of undoped CdTe crystals with high electrical resistivity, J.Crystal Growth 149 (1995) 201.
- [8] P. Rudolph, K. Shimamura, T. Fukuda, The radial selectivity of in-situ core-doped crystal rods grown by the double-die EFG method, Crystal Res.Technol. 29 (1994) 801.
- [9] T. Fukuda, P. Rudolph, S. Uda (eds.), Fiber Crystal Growth from the Melt, Ser. Adv. in Materials Res. 6 (Springer, Berlin 2004).
- [10] W. Miller, Ch. Frank-Rotsch, M. Czapalla, P. Rudolph, Numeric modeling of Czochralski growth of quadratic silicon crystals by means of TMF, Cryst. Res. Technol. 47 (2012) 285.
- [11] K.A. Jackson, D.R. Uhlmann, J.D. Hunt, On the nature of crystal growth from the melt, J. Crystal Growth 1 (1967) 1.

- [12] F.M. van Bouwelen, W.J.P. van Enckevort, A simple model to describe the anisotropy of diamond polishing, *Diamond and Related Materials* 8 (1999) 840.
- [13] P. Rudolph, M. Czupalla, B. Lux, F. Kirscht, Ch. Frank-Rotsch, W. Miller, M. Albrecht, The use of heater-magnet module for Czochralski growth of PV silicon crystals, *J. Crystal Growth* 318 (2012) 249.
- [14] A.F. Ioffe, A.R. Regel, Non-crystalline, amorphous and liquid electronic semiconductors, *Prog. Semicond.* 4 (1960) 237.
- [15] V.M. Glazov, S.N. Chizevskaya and N.N. Glagoleva, *Liquid Semiconductors* (Plenum, New York, 1969).
- [16] A.A. Chernov, Notes on interface growth kinetics 50 years after Burton, Cabrera and Frank, *J. Crystal Growth* 264 (2004) 499.
- [17] P. Rudolph, H.J. Koh, N. Schäfer, T. Fukuda, The crystal perfection depends on the superheating of the mother phase too - experimental facts and speculations on the "melt structure" of semiconductor compounds, *J. Crystal Growth* 166 (1996) 578.
- [18] M. Mühlberg, P. Rudolph, M. Laasch, E. Treser, The correlation between superheating and supercooling in CdTe melts during unseeded Bridgman growth, *J. Crystal Growth* 128 (1993) 571.
- [19] P. Rudolph, M. Mühlberg, Basic Problems of Vertical Bridgman Growth of CdTe, *J. Mat. Sci. Engin. B* 16 (1993) 8.
- [20] P. Brunet, A. Katty, D. Schneider, A. Thomson-Carli, R. Triboulet, Horizontal Bridgman growth of large high quality Cd_{1-y}Zn_yTe crystals, *Mat. Science Eng. B* 16 (1993) 44.
- [21] M.P. Kulakov, V.D. Kulakovskii, A.V. Fadeev, Twinning in ZnSe crystals grown from the melt under pressure, *Inorg. Mater.* 12 (1975) 1536.
- [22] P. Rudolph, Fundamental studies on Bridgman growth of CdTe, *Progr. Crystal Growth Charact. Mat.* 29 (1994) 275.
- [23] L. Shcherbak, P. Feichouk, O. Panchouk, Effect of CdTe "postmelting", *J. Crystal Growth* 161 (1996) 1.
- [24] J.-P. Gaspard, J.-Y. Raty, R. Uolin, R. Bellissent, Local orders in II-VI liquid compounds, *J. Non-Crystalline Solids* 205-207 (1996) 75.
- [25] S. Dalgic, M. Colakogullari, The structural properties of the liquid CdTe based on Reverse Monte Carlo modelling, *J. Non-Crystalline Solids* 353 (2007) 1936.
- [26] Ch. Henager Jr., J.R. Morris, Atomistic simulation of CdTe solid-liquid coexistence equilibria, *Phys. Rev. B* 80 (2009) 245309.
- [27] Yadong Xu, Wanqi Jie, P.J. Sellin, Tao Wang, Li Fu, Gangqiang Zha, P. Veeramani, Characterization of CdZnTe crystals grown using a seeded modified vertical Bridgman method, *IEEE Transactions on Nuclear Science* 56 (2009) 2808.
- [28] E. Saucedo, P. Rudolph, E. Dieguez, Modified Bridgman growth of CdTe crystals, *J. Crystal Growth* 310 (2008) 2067.
- [29] R. Triboulet, Crystal growth by traveling heater method, in: T. Nishinaga, P. Rudolph, T. Kuech (eds.), *Handbook of Crystal Growth, Second Edition, Vol. IIA* (Elsevier, Amsterdam 2015) pp. 459.
- [30] H. Shiraki, M. Funaki, Y. Ando, Sh. Kominami, K. Amemiya, R. Ohno. Improvement of the productivity in the growth of CdTe single crystal by THM for the new PET system, *IEEE Trans. Nucl. Sci.* 56 (2009) 1717.
- [31] J. Mackenzie, F.J. Kumar, H. Chen, Advancements in THM-Grown CdZnTe for use as substrates for HgCdTe, *J. Electron. Mater.* 42 (2013) 3129.

- [32] K.Schwenkenbecher, P.Rudolph, Investigation of convection in the solution zone at the growth of CdTe by THM, *Crystal Res.Technol.* 20 (1985) 1609.
- [33] P. Rudolph, P. Gille, Ch. Genzel, T. Boeck, Investigations of the Process of Crystal Growth from a Liquid Zone, *Crystal Res.Technol.* 19 (1984) 1073.
- [34] P. Gille, M. Mühlberg, L. Parthier, P. Rudolph, Crystal growth of PbTe and (Pb, Sn)Te by the [Bridgman method and by THM, *Crystal Res.Technol.* 19 (1984) 881.
- [35] P. Rudolph, Defect formation during the crystal growth from melt, in: G. Dhanaraj, K. Byrappa, V. Prasad, M. Dudley (eds.), *Springer Handbook of Crystal Growth* (Springer Verlag, Berlin 2010) pp. 153.
- [36] P. Rudolph, Non-stoichiometry related defects at the melt growth of semiconductor compound crystals - a review, *Crystal Res. Technol* 38 (2003) 542.
- [37] P. Rudolph, M. Neubert, M. Mühlberg, Defects in CdTe Bridgman monocrystals caused by non-stoichiometric growth conditions, *J.Crystal Growth* 128 (1993) 582.
- [38] P. Rudolph, H. Schröter, U. Rinas, H. Zimmermann, R. Boyn, The control of stoichiometry and substitutional acceptor density during crystal growth of CdTe, *Adv. Mat. for Optics and Electron.* 3 (1993) 289.
- [39] P. Rudolph, U. Rinas, K. Jacobs, Systematical steps towards exact stoichiometric and uncompensated CdTe Bridgman crystals, *J. Crystal Growth* 138 (1994) 249.
- [40] P. Rudolph, S. Kawasaki, S. Yamashita, S. Yamamoto, Y. Usuki, Y. Konagaya, S. Matada, T. Fukuda, Attempts to growth of undoped CdTe crystals with high electrical resistivity, *J. Crystal Growth* 161 (1996) 28.
- [41] T. Fukuda, K. Umetsu, P. Rudolph, H.J. Koh, S. Iida, H. Uchiki, N. Tsuboi, Growth and characterization of twin-free ZnSe single crystals by the vertical Bridgman method, *J. Crystal Growth* 161 (1996) 45.
- [42] M. Neubert, P. Rudolph, Growth of semi-insulating GaAs crystals in low temperature gradients by using the vapour pressure controlled Czochralski method (VCz), *Progr. Crystal Growth Charact. Mat.* 43 (2001) 119.
- [43] Ching-Hua Su, Partial pressure of Cd in equilibrium with stoichiometric melt and solid of $Cd_{0.8}Zn_{0.2}Te$ between 300 °C and 1250 °C for melt growth, *J. Crystal Growth* 596 (2022) 126837.
- [44] M. Neubert, P. Rudolph, Ch. Frank-Rotsch, M. Czupalla, K. Trompa, M. Pietsch, M. Jurisch, St. Eichler, B. Weinert, M. Scheffer-Czygan, Crystal growth by a modified vapour pressure controlled Czochralski (VCz) technique, *J. Crystal Growth* 310 (2008) 2120.
- [45] F.-M. Kiessling, M. Albrecht, K. Irmscher, M. Roßberg, P. Rudolph, W. Ulrici, R. Fornari, Boron- and stoichiometry-related defect engineering during B_2O_3 -free GaAs crystal growth, *Physica Status Solidi C* 6 (2009) 2778.
- [46] P. Rudolph, M. Jurisch, Bulk growth of GaAs - an overview, *J. Crystal Growth* 198/199 (1999) 325.
- [47] E.Pfeifer, Untersuchungen zur Optimierung der Züchtungstechnologie von Bleimolybdat-Einkristallen nach der Czochralski-Methode, PhD-Thesis, Humboldt- University of Berlin 1990.
- [48] Shi Yanlei, Sun Niefeng, Xu Chengyan, Wang Shujie, Lin Peng2, Ma Chunlei, Xu Senfeng, Wang Wei, Chen Chunmei, Fu Lijie, Shao Huimin, Li Xiaolan, Wang Yang, Qin Jingkai, Thermal field of 6-inch indium phosphide single crystal growth by semi-sealed Czochralski method, *J. Inorganic Mat.* 38 (2023) 335.
- [49] L.P. Kubin, *Dislocations - Mesoscale Simulations and Plastic Flow* (Oxford University Press, Oxford 2013).

- [50] H. Klapper, P. Rudolph, Defect generation and interaction during crystal growth, in: P. Rudolph (ed.), *Handbook of Crystal Growth Second Edition Vol. IIB* (Elsevier, Amsterdam 2014) pp. 1093.
- [51] P. Rudolph, Dislocation patterning in semiconductor compounds, *Crystal Res. Technology* 40 (2005) 7.
- [52] P. Rudolph, Fundamentals and engineering of defects, *Progr. Crystal Growth Charact. Mat.* 62 (2016) 89.
- [53] P. Rudolph, Dislocation patterning and bunching in crystals and epitaxial layers - a review, *Crystal Res. Technol.* 52 (2017) 1.
- [54] R.J. Amodeo, N.M. Ghoniem, Dislocation dynamics. I. A proposed methodology for deformation micromechanics, *Phys. Rev. B* 41 (1990) 6958.
- [55] M. Naumann, P. Rudolph, M. Neubert, J. Donecker, Dislocation studies in VCz GaAs by laser scattering tomography, *J. Crystal Growth* 231 (2001) 22.
- [56] T. Tuomi, L. Knuutila, J. Riikonen, P.J. McNally, W.-M. Chen, J. Kanatharana, M. Neubert, P. Rudolph, Synchrotron X-ray topography of undoped VCz GaAs crystals, *J. Crystal Growth* 237 (2002) 350.
- [57] Ch. Frank-Rotsch, U. Juda, F.-M. Kiessling, P. Rudolph, Dislocation patterning during crystal growth of semiconductor compounds (GaAs), *Mat. Sci. Technol.* 21 (2005) 1450.
- [58] M. Kurz, A. Pusztai, G. Müller, CrysVUN++, a powerful computer code for global thermal modelling of industrial crystal growth processes, in: H.J. Bungartz, F. Durst, C. Zenger (eds), *High Performance Scientific and Engineering Computing. Lecture Notes in Computational Science and Engineering*, Vol 8. (Springer, Berlin, Heidelberg 1999) pp. 255 .
- [59] U. Juda, Ch. Frank-Rotsch, P. Rudolph, Analysis of dislocation cell patterns in as-grown compound materials (GaAs, CaF₂), *J. Mater. Sci: Materials in Electronics* 19 (2008) 342.
- [60] S.V. Raj, G.M. Pharr, A compilation and analysis of data for the stress dependence of the sub-grain size, *Mater. Sci. Eng.* 81 (1986) 217.
- [61] P. Rudolph, F.-M. Kiessling, Growth and characterization of GaAs crystals produced by the VCz method without boric oxide encapsulation, *J. Crystal Growth* 292 (2006) 532.
- [62] I. Hähnert, M. Mühlberg, H. Berger, Ch. Genzel, Study of the defect structure of CdTe-rich II-VI single crystals, *J. Crystal Growth* 142 (1994) 310.
- [63] P. Rudolph, K. Kakimoto, Crystal growth from melt under external force fields, *MRS Bulletin* Vol. 34, No. 4 (2009) 251.
- [64] P. Rudolph, Travelling magnetic fields applied to bulk crystal growth from the melt: the step from basic research to industrial scale, *J. Crystal Growth* 310 (2008) 1298.
- [65] Ch. Frank-Rotsch, N. Dropka, Fr.-M. Kießling, P. Rudolph, Semiconductor Crystal Growth under the Influence of Magnetic Fields, *Crystal Research and Technology* 55 (2) (2020) 1900115.
- [66] N.V. Abrosimov, A. Lüdge, H. Riemann, W. Schröder, Lateral photovoltage scanning (LPS) method for the visualization of the solid-liquid interface of Si_{1-x}Ge_x single crystals, *J. Crystal Growth* 237–239 (2002) 356.
- [67] Ch. Frank-Rotsch, P. Rudolph, Vertical gradient freeze of 4 inch Ge crystals in a heater-magnet module *J. Crystal Growth* 311 (2009) 2294.
- [68] H. Bitterlich, Ch. Frank-Rotsch, W. Miller, U. Rehse, P. Rudolph, Homogeneous TMF melt-solution mixing during dipping LPE of (Hg,Cd)Te layers, *J. Crystal Growth* 318 (2011) 1034.
- [69] Ch. Kudla, A. T. Blumenau, F. Büllsfeld, N. Dropka, Christiane Frank-Rotsch, F. Kiessling, O. Klein, P. Lange, W. Miller, U. Rehse, U. Sahr, M. Schellhorn, G. Weidemann, M. Ziem, G. Bethin, R. Fornari, M. Müller, J. Sprekels, V. Trautmann, P. Rudolph, Crystallization of 640 kg

mc-silicon ingots under traveling magnetic field by using a heater-magnet module, J. Crystal Growth 365 (2013) 54.

[70] E. Scheil, Bemerkungen zur Schichtkristallbildung, Zs. für Metallkunde 34 (1942) 70.